DESERT

Desert
Online at http://desert.ut.ac.ir

Desert 25-2 (2020) 185-199

Soil temperature modeling using machine learning techniques

S. Fathololoumi[a,b*], A.R. Vaezi[a], S.K. Alavipanah[c,d], C. Montzka[e], A. Ghorbani[b], A. Biswas[f*]

[a] *Department of Soil Science, Faculty of Agriculture, University of Zanjan,Zanjan, Iran*
[b] *Faculty of Agriculture and Natural Resources, University of Mohaghegh Ardebili, Ardabil, Iran*
[c] *Department of Remote Sensing and GIS, University of Tehran, Tehran, Iran*
[d] *Department of Geography, Humboldt University Berlin, Berlin, Germany*
[e] *Forschungszentrum Jülich, Institute of Bio- and Geosciences: Agrosphere (IBG-3), 52428 Jülich, Germany*
[f] *School of Environmental Sciences, University of Guelph, Canada*

Received: 19 February 2020; Received in revised form: 20 April 2020; Accepted: 5 May 2020

Abstract

Soil Temperature (ST) is critical for environmental applications. While its measurement is often difficult, estimation from environmental parameters has shown promise. The purpose of this study was to model ST in cold season from soil properties and environmental parameters. This study was conducted as a pot experiment in Ardebil, Iran. Automatic thermal sensors were installed at 5 and 10 cm depths. Besides, soil properties and environmental parameters were determined based on field and laboratory works. Machine learning methods including Multiple Linear Regression (MLR), Artificial Neural Network (ANN), and Adaptive Neuro-Fuzzy Interface System (ANFIS) were used for modeling ST. The air temperature was observed as the most effective factor in ST modeling. The relationship between soil and air temperature was stronger at 5 cm depth compared to 10 cm. The R^2 between soil and air temperature was higher in the absence of sunlight than in its presence. The prediction of ANFIS (R^2= 0.96 and MAPE= 10.5) was closer to the observed ST values compared to the ANN (R^2= 0.91 and MAPE= 35) and MLR (R^2= 0.57 and MAPE= 41). The results revealed the advantage of ANFIS method for ST modeling. This approach can be applied for soil depths and locations with data gap.

Keywords: Environmental parameters, Modeling, Shadow, Soil properties

1. Introduction

Soil temperature (ST) reflects the amount of radiation emitted from the surface and sub-surface of the earth and determines the exchange of energy between Earth's surface and atmosphere (Weng *et al.*, 2019a). It is one of the most important parameters affecting climate change (Davidson and Janssens, 2006). Soil temperature is a key factor in Soil Moisture (SM) retrieval, determination of ST regimes, soil organic matter decomposition rate, seed germination, and plant growth (Moore *et al.*, 2015; Sandholt *et al.*, 2002; Shaoning *et al.*, 2014). Soil temperature fluctuations over time and in space is among the most important factors affecting the exchange and transport of matter and energy and direct or indirect physical processes in the soil (Gao *et al.*, 2017; Onwuka and Mang 2018; Wang *et al.*, 2014; Weng *et al.*, 2019a).

Soil temperature regimes and distribution of temperature profiles depend on the terrain, meteorological, and subsurface variables (Hartemink and Bockheim, 2013; Stolpe and Undurraga, 2016). These variables include the structure and physical properties of Earth's surface and its thermal properties, vegetation coverage, SM, and climatic variables including temperature, rainfall, wind, solar radiation, and air humidity (Oyeyemi *et al.*, 2018; Weng *et al.*, 2019a). Solar radiation is one of the most important factors daily and seasonally affecting ST. Also, the local variations of ST are

* Corresponding author. Tel.: +98 914 1531831
Fax: +98 21 61112591
E-mail address: fathololomi.s@znu.ac.ir

associated with meteorological factors such as Air Temperature (AT), relative humidity, rain, and wind (Weng *et al.,* 2019a). As a result, the individual patterns of these characteristics generate unique ST patterns (Mojarrad and Sadeghi, 2013). Recent studies have shown that the mean AT of Earth increased by 0.8 ˚C during 1906-2012 (Firozjaei *et al.,* 2019b). Therefore, information on ST changes is critical for studies related to climate changes, SM, soil properties, and plant growth (Weng *et al.,* 2019b).

Despite the importance of ST, the measurement costs, equipment requirement, and manpower restrict the data collection. Soil temperature data are usually sparse because their measurement is limited, especially in the subsurface. To fill the gap, the meteorological data are often used to estimate the ST, which may not be very accurate (Ozturk *et al.,* 2011). Data of such ilk may not be available in all regions. Therefore, it is important to develop models that are capable of accurately and quickly predicting ST and its fluctuations. However, it is scientifically important to specify the best combination of the most important independent variables. It is also necessary to develop models with the least number of effective parameters as model inputs.

Many methods such as Fourier series (Carter and Ciolkosz, 1980; Ghuman and Lal, 1989), linear and nonlinear regressions (Bilgili 2010), sinusoidal models (Lei *et al.,* 2011), artificial intelligence (Singh *et al.,* 2018), Gaussian process regression (Mihoub *et al.,* 2016), soil-landscape regression (Tsai *et al.,* 2001), machine learning algorithms (Delbari *et al.,* 2019), and energy balance equations (Weng *et al.,* 2019a) were used to model ST at the surface and at different depths. Each of these methods offers advantages and disadvantages for ST modeling. Nowadays, Artificial Intelligence (AI) techniques such as Artificial Neural Networks (ANNs), fuzzy logic, neuro-fuzzy, and Adaptive Neuro-Fuzzy Interface System (ANFIS) (Feng *et al.,* 2019; Sanikhani *et al.,,* 2018) have attracted a great deal of attention in various scientific applications (Pelletier *et al.,,* 2016) such as ST modeling (Bonakdari *et al.,,* 2019; Sanikhani *et al.,,* 2018; Yener *et al.,,* 2017). Maduako *et al.* (2016) modeled ST using remotely sensed data and ANN method. They used Feed Forward Back Propagation (FFBP) method and showed its reasonable accuracy in ST modeling.

Some of these studies used soil properties data to model ST (Knight *et al.,* 2018; Luo *et al.,* 2018) while others employed AT and remotely sensed data (Florides and Kalogirou 2007; Maduako *et al.,* 2016; Şahin *et al.,* 2012). Delbari *et al.* (2019) utilized support vector regression (SVR) to estimate daily ST at 10, 30, and 100 cm soil depths. They used the data of three meteorological stations related to different climates in Iran. They compared the model results with multiple linear regression (MLR) results and reported that these two models provided a good prediction of daily ST in soil surface, and SVR performance was better in deep layers. Using 30 years of air and soil temperature data, Barman *et al.* (2017) predicted ST at 5, 15, and 30 cm depths. They used exponential and power regression models to model ST in the morning and afternoon. Exponential models had good predictions at both times. They concluded that the inclusion of AT was able to improve model performance. ANN and co-active ANFIS were used for ST modeling at 5, 10, 20, 30, 50, and 100 cm soil depths with 14 years of meteorological data as model input. The performance of both models was better in arid regions and the accuracy of both models decreased from the surface to deep layers (Abyaneh *et al.,* 2016).

Based on literature review, long time temperature data are required for ST modeling, possibly restricting the modeling in most situations (Bilgili, 2010). This is because there are not enough meteorological and synoptic stations to record ST, especially in mountainous areas and steep slopes. Therefore, providing ST data is a challenge in such areas. On the other hand, certain stations are newly established and do not have a strong regional database; thus, researchers may not be able to obtain the data they need for ST modeling. The current paper addresses this gap through modeling ST by use of short time in-situ ST data recorded by automatic thermal sensors. Moreover, according to literature review in previous studies, we did not consider the impact of soil properties such as soil texture on ST. Similarly, none of the mentioned studies accounted for the impact of shadow and sunshine on the accuracy of ST modeling at the surface and at depths despite their strong influence.

Given these research gaps, the purpose of this study was to model ST using short time air and soil temperature data, soil properties, and environmental parameters in cold season using regression and machine learning algorithms. The cold season was considered because ST data were not widely available in the hot season; also, to study the effect of environmental conditions such as air temperature on ST at different depths, the use of cold season data was more appropriate owing to the low impact of solar radiation on ST. The most important distinction between this

study and the previous ones is that we considered the effect of shadow and sun on modeling ST at the surface and sub-surface. Furthermore, for the first time, we used real short time ST data and measured SM in permanent shadow and sunlight to simultaneously investigate the effect of shadow, sun light, and moisture content. The relationship between soil and air temperature was also studied at two depths and two times of day (12 pm and 1 am) based on different soil textures and one manure sample.

2. Materials and Methods

2.1. Soil properties

Three types of soil texture classes, namelycoarse (sandy), medium (loam), and relatively fine (clay loam) were collected from Ap horizon (0-30 cm). To study the effect of organic matter on ST, a sample of livestock manure was used in this study. The texture, color, and bulk density (BD) were determined using hydrometer method (Klute and Dirksen 1986), Munsell color system (Pegalajar *et al*., 2018), and core method (Beretta *et al.,* 2014), respectively. Saturated hydraulic conductivity (Ks), pH, electrical conductivity (EC), and calcium carbonate equivalent (CCE) of different soil types of were measured using constant head method (Wang and Benson 2018), saturated paste, 1:2.5 (sample: water) suspension (Jackson, 2005), and the method described in (Nelson, 1982), respectively. The samples were transferred to eight plastic containers of 33×25×20 cm (length × width × height) size. The present study was conducted as a pot experiment in Ardebil, Iran. The geographical location of experiment was 38° 14' 12.75″ N and 48° 16' 46.75″ E (Figure 1). The containers were filled with respective soil samples according to their natural conditions in the field. In all samples, the initial SM was 30% by volume. We prepared two sets of experiments consisting of four containers filled with four soil types. Each container was equipped with RC-5 automatic thermal sensors (Elitech UK, Figure 1b) at 5 and 10 cm depths, and the ST was recorded for 53 days with 10 min intervals.

Daily soil sampling was conducted for gravimetric SM measurement during the experimental phase. To prevent destructive effects on soil, sampling was carried out in another container prepared alongside the original boxes and under the same conditions as the original boxes. After 53 days (from December 22 to February 12, 2018), the final SM of the experiment boxes was measured by gravimetric method. Additionally, the soil organic matter (OC) was measured based on Walkley-Black method (Nelson and Sommers, 1982).

2.2. Environmental (meteorological) characteristics

Based on the literature, environmental characteristics such as air temperature (Onwuka and Mang, 2018; Zhang *et al.,* 2015) were further selected as model inputs. The AT was measured by two automatic thermal sensors installed on top of the containers (two meters above the surface) (Figure 1a). To study the effect of sunlight and shadow on ST, two sets of similar containers were used. The first set (four containers) was placed under permanent sunshine, and the second set (four containers) was positioned under permanent shadow (Figure 1b).

During the experiment time, the minimum and maximum ATs were -2.9 and 10 °C, respectively. The relative air humidity was 72.66 % and the total solar time was 293 hours, which was representative of the cold weather conditions inthe region. The total precipitation was 71.3 mm during the experiment time.

2.3. Fluctuations in air and soil temperature

Previous studies showed the relationship between ST and AT (Koçak *et al.*, 2004). Similarly, ST depends on the soil depth and time of day and year (Yener *et al.,* 2017). We recorded air and soil temperatures at different depths and different times of day to investigate the diurnal variations and their relationship with other soil properties. We also studied the correlation between ST and AT at different depths and soil types. The R^2 values were calculated to quantitatively study their association. AT was plotted against ST at 5 and 10 cm depths at two times of day in the presence (12 pm) and absence of sunshine (1 am).

2.4. ST modeling based on soil properties and environmental parameters

Air temperature (AT), SM, BD, sun (sun-shadow) (S), soil depth (D), day per year (DA), and hour per day (T) were included as independent variables to predict ST. The ST measured at different depths was also considered as dependent variable. Three different algorithms, namely MLR, ANN, and ANFIS networks, were employed for ST modeling.

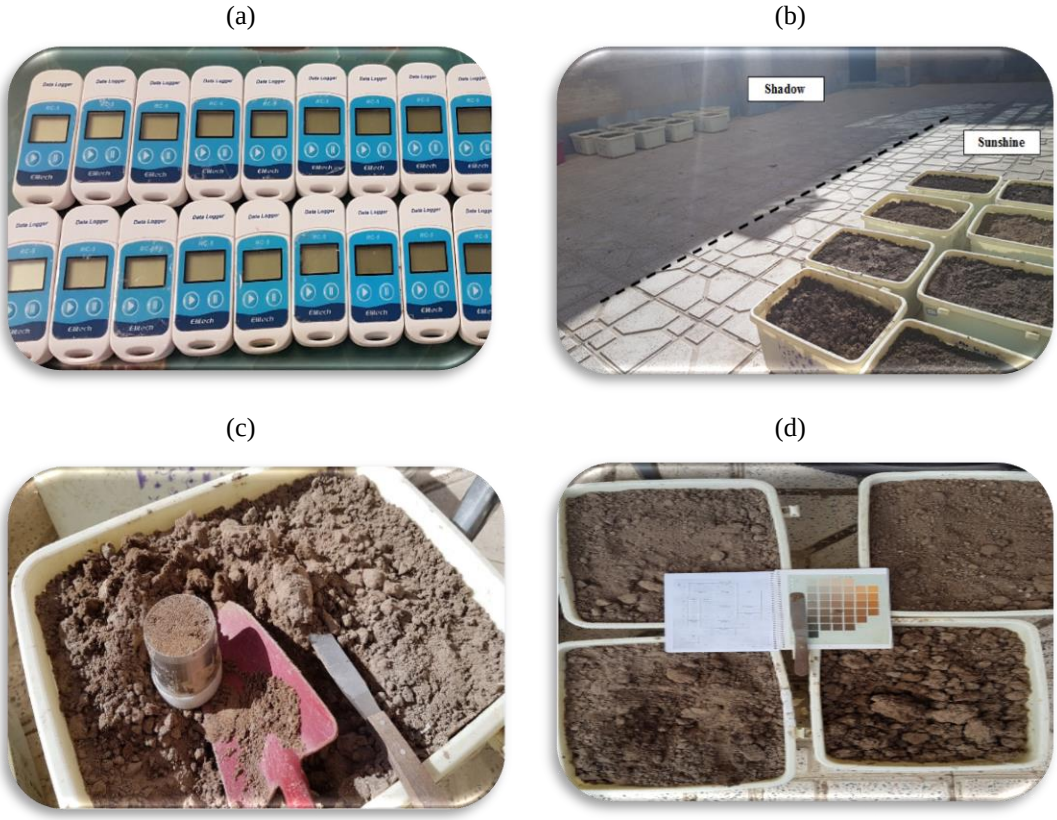

Fig. 1. Automatic thermal sensors used in the research: (a) placing the containers in two sections (shadow and sunlight), (b) sampling for BD determination (c), specifying the soil color (d)

2.4.1. MLR

Regression analysis is a statistical method for modeling the relationship between variables. Several kinds of regression, including linear, multiple, and nonlinear regression are employed in statistical analysis (Chatterjee and Hadi, 2015; Seber and Lee, 2012). Multiple linear regression (MLR) was used in this study to examine the impact of soil properties and environmental parameters on ST and its modeling. MLR can determine the influence of soil properties and environmental parameters on ST. This method was selected owing to its simple and easy implementation, low processing volume, clear processing and output process while artificial intelligence methods are black box. However, various studies have reported that the relationship among ST, soil properties, and environmental parameters is rather complex (Bonakdari *et al.*, 2019; Abyaneh *et al.*, 2016). Therefore, the relationship of soil properties and environmental parameters with ST may be nonlinear under various conditions, in which case artificial intelligence methods could be useful.

2.4.2. ANN

In ANN networks, the input and output values are related to one another(Singh *et al.*, 2018). Multilayer networks are very powerful and can estimate any arbitrary function with a finite number of discontinuities (Firat and Gungor, 2009). In the multilayer neural network, each layer has its own weight matrix, bias vectors, and outputs. The outputs of each middle layer are utilized as the next layer inputs. Having a hidden layer with sigmoid function in the middle layer and linear function in the output layer, ANN is able to approximate all the desired functions with any degree of approximation providedthere are sufficient neurons in the hidden layer (Bilgili, 2010; Hecht-Nielsen, 1992). In the present study, a multi-layer perceptron ANN was employed with an error post-propagation algorithm, a perceptron network with a hidden layer tangent function, and a linear transfer function (purelin) for the output neuron. To implement the model,

the collected data were randomly divided into three sections with 70% of the samples as training, 15% as validation, and 15% as testing. Levenberg-Marquardt algorithm was employed for training.MATLAB R2014a toolbox was used to design the ANN method.

2.4.3. ANFIS

ANFIS technique is a hybrid method having the advantages of both ANN and Fuzzy logic (Walia *et al.*, 2015). In this study, the ANFIS network contained five layers with several nodes and was described by the node function. In layer one, every node was an adaptive node with a node function such as a generalized bell or a Gaussian membership function. In layer two, each node multiplied the incoming signals and the output was a product of all the incoming signals. Each node output represented the firing strength of a rule. In layer three, each node calculated the ratio of the i^{th} rule's firing strength to the sum of all rules' firing strengths. The normalized firings were the output of this layer. In layer four, each node calculated the contribution of the i^{th} rule to the overall output. In layer five, one single node calculated the final output as the summation of all input signals (Karthika and Deka, 2015). The grid partition and sub-clustering structure were used to create the ANFIS network. In grid partition, the range of each input was divided into equal intervals; one rule was created in each multidimensional space resulting from the combinations of different inputs. Four types of membership function (triangular, trapezoid, Gaussian, and bell-shaped) were considered to represent the inputs (Figure 2). Output membership functions in both network structures were linear. Hybrid optimization method was used for network training. Several rules and a predictive linear function were created by ANFIS (Table 3), and different values were modeled (Figure 3). At this stage, the weight of each rule was determined based on the entry degree of the input signal in the membership functions for each variable. To implement the model, the collected data were randomly divided into two sections where 70% of the samples were assigned to training and 30% to testing the model. The final modeled values were determined from Eq. (1) (Buragohain and Mahanta, 2008).

$$f = \frac{w_1 f_1 + w_2 f_2}{w_1 + w_2} \quad (1)$$

where f_1 and f_2 are the linear functions of rules 1 and 2, and w_1 and w_2 are the weights corresponding to each rule, respectively.

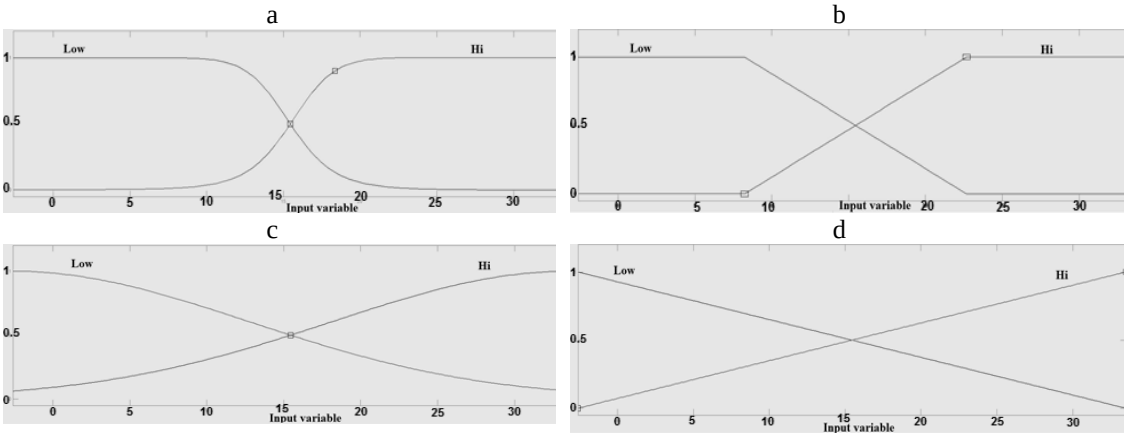

Fig. 2. Primitive sample membership functions of input variables: (a) bells, (b) trapezoidal, (c) Gaussian, and (d) triangular. The X and Y axes show the input variables and membership degree of input variables, respectively. The lines indicate the membership functions

2.5. Accuracy assessment

To evaluate the ability of the models to model ST and determine the performance of each approach, the statistical criteria related to the coefficient of determination (R^2) and Mean Absolute Percentage Error (MAPE) were used (Eqs. (2) and (3)) (Carman, 2008; Jacovides, 1998):

$$R^2 = 1 - \frac{\sum_{i=1}^{N}(\mathrm{Y_{measured}} - \mathrm{Y_{modeled}})^2}{\sum_{i=1}^{N}(\overline{\mathrm{Y}}_{\mathrm{measured}} - \mathrm{Y_{modeled}})^2} \quad (2)$$

$$\mathrm{MAPE} = \frac{100\%}{\mathrm{N}} \sum_{\mathrm{i=1}}^{\mathrm{n}} \frac{\mathrm{Y_{measured}} - \mathrm{Y_{modeled}}}{\mathrm{Y_{measured}}} \quad (3)$$

where N, $Y_{modeled}$, and $Y_{measured}$ are the number of samples, modeled values, and measured values, respectively. $\overline{Y}_{measured}$ is the mean of the measured values.

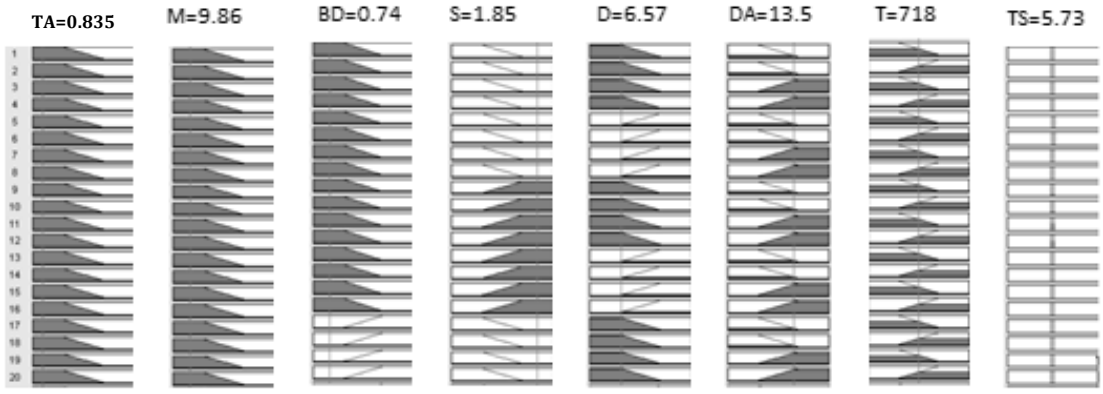

Fig. 3. ANFIS rules viewer and rules of the ST models. The grey signs indicate the range of input variables. Upper values such as TA= 0.835 are random numbers which we entered into the model to assess its capability in ST modeling. The numbers next to the shape (1-20) are the rules number

3. Results and Discussion

3.1. Environmental (meteorological) characteristics and soil properties

The minimum and maximum recorded ST were 30 and 60 °C, respectively; the total number of ST data recorded for each soil type was 5759. The highest BD belonged to the sandy soil (1.85 g cm^{-3}), and the lowest value was detected in the clay loam soil (1.25 g cm^{-3}) (Table 1). Due to the presence of more aggregates and pores, the BD of clay loam soil was lower than sandy soil (Daddow and Warrington, 1983). Due to the proximity of the particles and the reduction in the pores between them, BD was higher in the sandy soil (Chaudhari *et al.,* 2013). The highest and lowest Ks values were related to sandy soil (2.59 cm min^{-1}) and clay loam soil (0.09 cm min^{-1}), respectively. Ks values are directly affected by pore size which was higher in the sandy soil (Ren and Santamarina, 2018). The manure sample had the smallest pH (5.5) and was more acidic than the soil samples. It had the highest EC (11.2 ds m^{-1}) in comparison with other soil samples. Clay loam soil had the highest CCE, which can be attributed to the role of the clay minerals in the absorption of elements such as calcium and their availability (Kome et al., 2019). Among soil samples, the maximum and minimum OC values were detected in clay loam and sandy soil, respectively, which is due to the ability of fine-textured soils in OC protection. As a result, OC content in clay loam soil was higher than coarse-textured soil which was sandy in this study (Hassink *et al.,* 1997) (Table 1).

Table 1. Characteristics of the studied soils and manure sample

Texture	*Sand (%)*	*Silt (%)*	*Clay (%)*	*Color*	*BD (g cm^{-3})*	*Ks (cm min^{-1})*	*pH*	*EC (ds m^{-1})*	*CCE (%)*	*OC (%)*
Sandy	90	8	2	7.5 YR 5/3	1.85	2.59	6.9	0.11	4.6	0.10
Loamy	44	38	18	7.5 YR 7/3	1.6	0.97	7.2	0.26	10.3	0.53
Clay Loam	36	26	38	5 YR 4/3	1.25	0.09	7.5	0.83	18.0	0.84
Manure	-	-	-	7.5 YR 3/2	0.64	2.13	5.5	11.2	0.0	29.42

3.2. Fluctuations in ST and AT

The decrease in AT reduced the ST in both depths (Figure 4). Generally, temperature changes play a special role in the natural environment (Liao and Huang, 2012). The variation range of ST in the soil surface was higher than the subsurface during the day. Also, because of the higher AT, the ST was greater throughout the day than night. The ST variation at 5 cm depth was higher than 10 cm. This means that by increasing the soil depth, the range of variations decreased, which is due to the lower impact of climatic parameters with the increase in soil depth (Parsafar and Marofi, 2011). Several studies have shown that there exists a delay in heat transfer in soil (Bi *et al.,* 2018; Park, 2018). These results are similar to some other findings (Liang *et al.,* 2014; Mojarrad and Sadeghi, 2013).

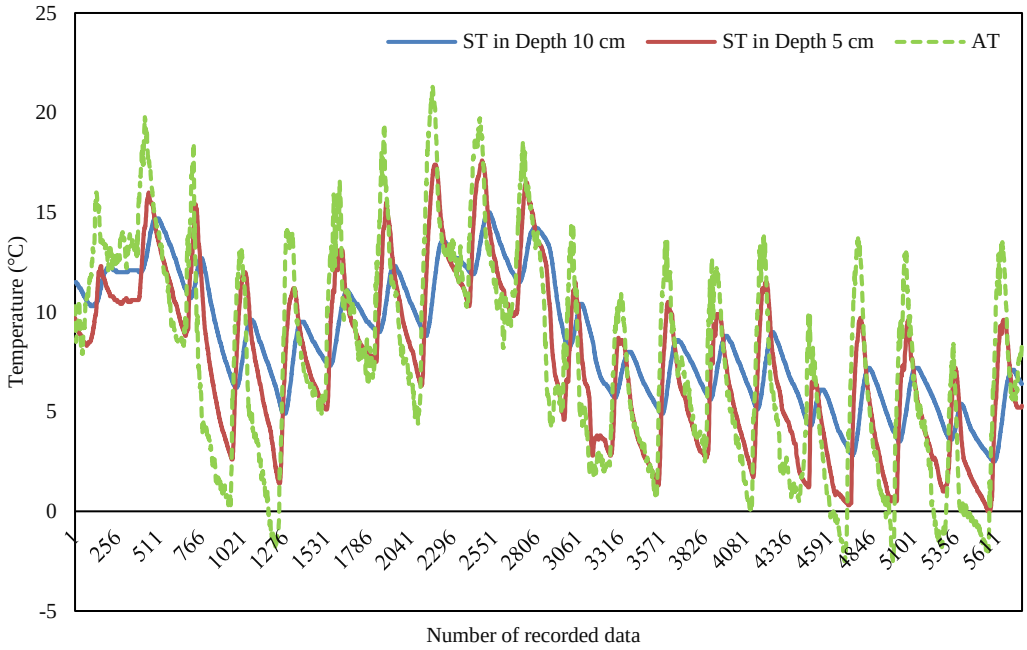

Fig. 4. Air and soil temperature fluctuations at 5 and 10 cm soil depth. This diagram is related to loamy soil as an example

Figure 5 depicts the diagrams of 5 cm (a) and 10 cm depths (b) for each soil type. Generally, soil type had no effect on the order of deep ST distribution in this study. This result is probably due to the low air temperature. When the temperature of the soil samples was higher than the average AT, the manure temperature was higher than soil samples at 5 cm depth. Meanwhile, when the temperature of the soils was lower than the average AT, the manure temperature was less than the soil samples at 5 cm depth (Figure 5a). This finding is probably attributed to the more water retention in the manure sample (Reeves, 1997).Owing to its sponge-like properties, organic matter has higher water holding capacity and absorption compared with soil samples. Moisture acts as a dielectric material in the soil and prevents sharp and sudden temperature changes. Accordingly, SM improves the heat balance during night and increases the heat storage and nocturnal ST. With the increase in moisture, the difference between day and night temperature decreases. This might also be attributed to the higher absorption of heat by organic matter (Onwuka and Mang, 2018) during the day and lower loosing of that during night in cold weather. These results are similar to the findings of Al-Kayssi *et al.* (1990); they reported a decrease in ST differences between daytime and nighttime as a result of moisture content increase. This positively affects plants when the soil has sudden temperature changes. The plant root system has been protected from sharp changes of ST by moisture effects on that. Also, higher SM increases solar energy absorption by the soil. Thus, heat storage capacity increased in wet soils, affecting the plant climate and plant growth in the soil, which is in line with Bilgili (2010) results. He concluded that the SM related to soil texturestrongly affects the temperature gradients. Another factor affecting ST is organic carbon (OC) which makes the soil color darker. Dark color causes more solar energy absorption, hence warmer soil. Moreover, the ST at both studied depths during night was higher than the AT (Figure 5). This result confirms the time delay in heat transfer in the soil (Li and Lai, 2012).

During the first few days of the experiment, the manure temperature variation was less than soil, probably due to the initial SM of the samples. The higher water holding capacity and higher SM storage in the manure contributed to a different thermal behavior (Oyeyemi *et al.*, 2018). This process was true for other samples as well. In the following days, on the other hand, SM content diminished under the influence of wind and sun. As a consequence, its temperature behavior changed compared to the first days.

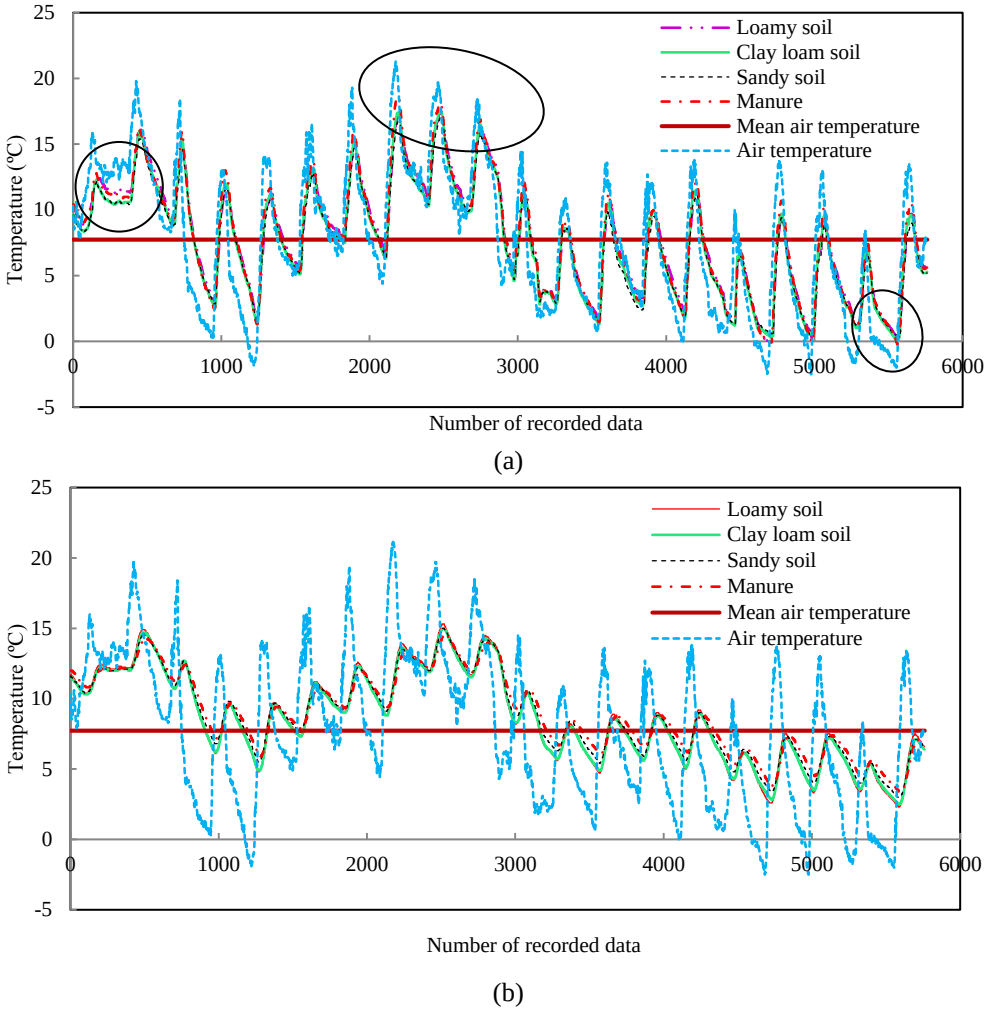

Fig. 5. Soil temperature at 5 cm (a) and 10 cm (b) depths in soils with different textures and in the manure sample. Some temperature variations in different samples are shown with three ovals on the graph (a)

The difference between the ST was more evident at 10 cm depth (Figure 5b). This might be attributed to the difference in heat conduction and heat transfer at different soil depths (Bilgili, 2010; Lu *et al.*, 2007). Due to the effect of the solar energy at the soil surface, heat transfer does not have an important role. Meanwhile, at the subsurface, the main determinant of ST is the intensity of heat transfer from the surface to the depth of the soil (Kupfersberger *et al.*, 2017; Quattrochi and Luvall, 2004). This was also confirmed by the visual survey of temperature curves (Figure 5b). As seen in the ST curves, the difference between the temperature of the experimental samples and the air temperature curves was higher at nighttime. This difference was especially greater in temperatures below the mean air temperature. Earth's surface temperature is affected by many environmental variables such as surface biophysical characteristics, topography parameters, solar radiation, AT, wind intensity, SM, and soil type (Alavipanah *et al.*, 2017; Oyeyemi *et al.*, 2018; Weng *et al.*, 2019a).

The thermal conductivity of the soil expresses the soil ability in heat conduction and is strongly affected by physical properties of the soil such as BD, SM content, and other soil physical properties (Rubio *et al.*, 2009). Different soil properties are among the most important factors controlling heat emission in the soil (Mojarrad and Sadeghi, 2013). We investigated the relationship between AT and the ST recorded at different depths and soil types. To this end, the R^2 values were calculated and the regression lines were plotted at both depths (Figure 6).

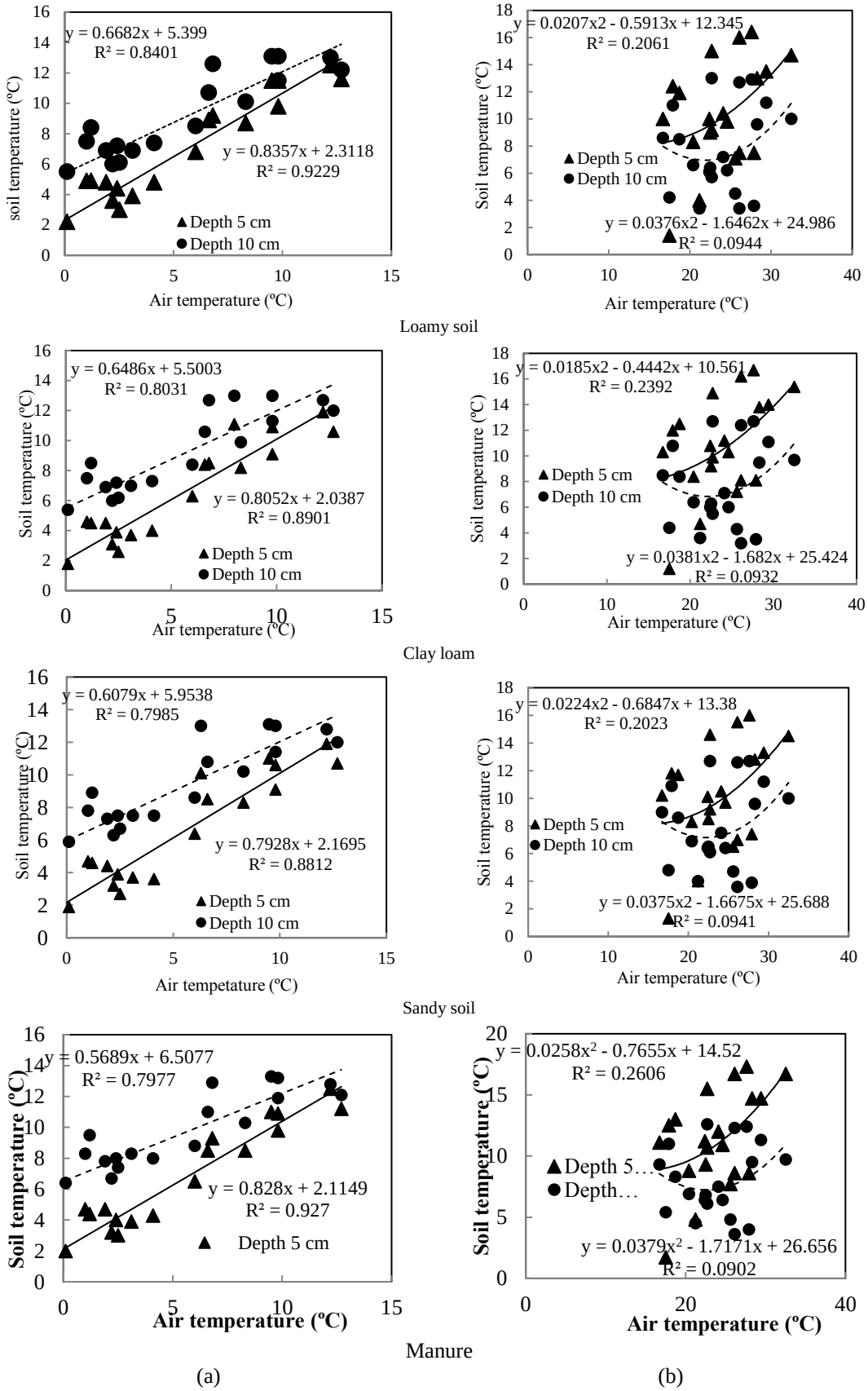

Fig. 6. Soil temperature at 5 and 10 cm depths at 12 pm (a) and 1 am (b) in different days during the experiment period and their correlation with AT

In all four samples (sandy, loamy, clay loam soils, and manure), the correlation between ST and AT was stronger at 1 am than 12 pm (Figure 6). The effect of solar radiation, AT fluctuations, time delay in heat, and soil fluctuations resulted in a lower correlation at 12 pm. However, at 1 am, the lack of solar radiation and the stability of the AT conditions resulted in a greater correlation between ST and AT. There was no significant difference between the samples in shadow and sun, possibly due to the cold weather and low AT.

As the manure bulk density was the lowest, minimum temperature changes in the manure sample and maximum temperature changes in sandy soil were expected (Angers and Chenu, 2018). With the increase in bulk density, the contact between the particles increased, subsequently augmenting the thermal conductivity (Lipiec and Hatano, 2003). The amount of heat dissipated through the manure surface increases with increasing the bulk density; this is because it increases the rate of heat energy passing through a unit cross-sectional area of the manure (Onwuka and Mang, 2018).

The large amount of organic matter reduced the brightness value of soil. The darkness of soil is due to the presence of high amounts of organic carbon. OC not only resulted in a significant absorption of solar radiation, but also decreased the temperature changes within the soil. The effects of OC are related to its inherent spongy microstructure (Ghuman and Lal, 1989; Terefe *et al.*, 2008). It also augments the water absorption capacity in the soil substrate (Rawls *et al.*, 2003). Therefore, manure was expected to have the lowest temperature variations in contrast to sandy soil with the lowest organic matter content as characterized by the highest temperature variations.

3.3. ST modeling based on machine learning algorithms

3.3.1. MLR

Air temperature, humidity, and soil physical properties could be effective predictors in estimating the subsurface temperature. The most significant aspect of MLR method is selecting the predictors of dependent variable prediction. Thus, all independent variables were added to the model as inputs. The MLR model output was as follows. The relationship between ST, as a dependent variable, and input factors to the MLR method was obtained for the cold season:

$$TS=8.38+0.333AT-.025DA+0.002T+0.705S-0.109M+0.163D-1.67BD \quad (4)$$

The regression model (Eq. 4) shows the importance and the effect of independent variables on dependent variable (ST); it also shows how independent variables can affect ST. Unlike ANN and ANFIS, MLR can provide information on the internal structure of the model and the relationship between independent and dependent variables.

According to the standardized coefficients (Eq. 4), AT, day, time, sun's state, moisture, depth, and BD had the most impact on the ST. The R^2 and MAPE values between the modeled ST and the observed ST (0.58 and 35, respectively) were used to assess the model performance. There was no statistically significant difference between the temperatures of the soils and different colors. This might be ascribed to the low temperature and low solar radiation of the sun during the research period. The amount of surface incoming solar radiation is lower in winter because of the smaller angle of landing (Allen *et al.*, 2006; Firozjaei *et al.*, 2019a; Kalogirou, 2013). This is possibly another reason that color had no effect on ST. The effect of SM on ST was negative, meaning with the increasing moisture content in the soil, the temperature decreased (Dai *et al.*, 1999). Depth and BD had positive effects where their increase augmented the ST.

3.3.2. ANN

The R^2 and MAPE between the observed and modeled ST using ANN were 0.91 and 15, respectively. These values indicate the better performance of ANN over the MLR method.

3.3.3. ANFIS

Several rules were created by ANFIS model along with a predictive linear function (Table 2).

The membership functions of all inputs for the first and second half of the information are represented by the letter S and B, respectively (Table 3). The first part in this network is in the form of Fuzzy rules (if-then), and the resultant section is non-Fuzzy in the form of a linear function consisting of input variables. The R^2 and MAPE for the best network and membership function of ANFIS were 0.96 and 10.5, respectively.

Table 2. The linear output functions (ST) and their input variables of AT, SM, BD, sun (sun- shadow) (S), soil depth (D), day (DA), and hour per day (T)

Linear output functions (ST)	Input Variables							Rules
	AT	SM	BD	S	D	DA	T	
ST= -0.1463AT+ 4.431SM+ 163.7BD -8.147S -40.74D+ 8.097DA -0.005851T -8.147	S	S	S	S	S	S	S	Rule No. 1
ST= 1.16AT -1.576SM+ 11.02BD+ 1.714 4.284S -1.07D -0.004912DA+ 0.8568T	S	S	S	B	S	S	B	Rule No. 10
ST= 0.2396AT+ 1.988SM+ 71BD -1.213S -12.13D+ 2.377DA -0.004891T -1.213	S	S	B	S	B	S	S	Rule No. 21
ST= 0.3627AT+ 0.8709SM+ 389.2BD -10.81S -54.03D+ 1.669DA -0.004402T -10.81	S	B	S	S	S	B	B	Rule No. 36
ST= 4.329AT -2.141SM -52.19BD+ 3.738S+ 18.69D+ 1.079DA -0.00833T+ 3.738	S	B	B	S	S	S	B	Rule No. 50
ST= -0.1712AT+ 13.9SM+ 34.28BD -3.29S -16.45D - 11.49DA+ 0.07315T -3.29	B	S	S	S	S	B	S	Rule No 67
ST= 0.4232AT -1.385SM -60.59BD+ 4.391S+ 21.96D - 4.139DA -0.008805T 4.391	B	S	B	S	S	S	S	Rule No. 81
ST= -1.861AT+ 18.53SM+ 1227BD -77.63S -388.1D+ 50.78DA -0.01226T -77.63	B	B	S	S	S	B	S	Rule No. 99
ST= 0.2269AT -0.5059SM+ 1110BD -3.971S -19.85D - 5.624DA -0.4056T -1.985	B	B	S	B	B	B	B	Rule No. 112
ST= -0.3293AT -17.95SM -488.2BD+ 82.33S+ 411.6D - 27.22DA -3.146T+ 41.16	B	B	B	B	B	B	B	Rule No. 128

Table 3. Characteristics and results of five types related to network and membership function of ANFIS for ST modeling

Type of network	Type of membership function		Number of membership functions	Optimization method	Results	
	Output	Input			R^2	MAPE
Grid Partition	Linear	Gbellmf	2-2-2-2-2-2-2	Hybrid	0.93	13.3
Grid Partition	Linear	Gaussmf	2-2-2-2-2-2-2	Hybrid	0.94	13.8
Grid Partition	Linear	Trimf	2-2-2-2-2-2-2	Hybrid	0.95	11
Grid Partition	Linear	Trapmf	2-2-2-2-2-2-2	Hybrid	0.96	10.5
Sub-clustering	Linear	Gaussmf	-	Hybrid	0.94	12.8

Among the different methods of ANFIS networks, the grid partition models had a higher R^2 than the sub-clustering models. However, their execution time to reach the constant error took longer, which can be attributed to the number of rules created in each of these states. Figure 7 shows the general structure of grid separation and the sub-clustering. The split-mode network had 128 rules and the sub-clustering regime had 71 rules. Many rules made the network more precise and sluggish. Such behavior has also been reported in other studies (Ay and Kisi 2014).

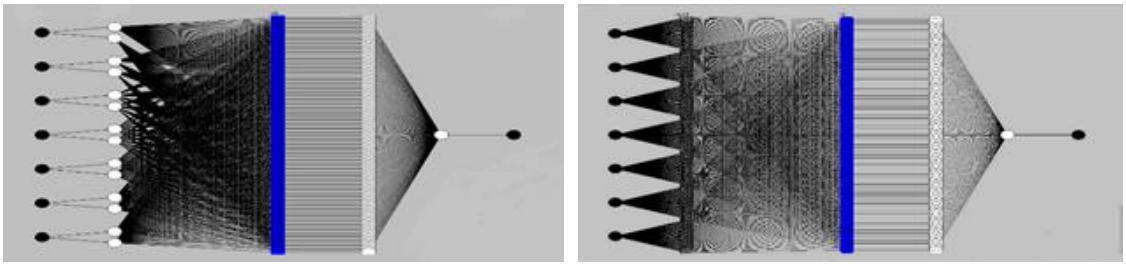

(a) (b)

Figure 7. Structure of the best ANFIS models for ST modeling: a) inference system with grid separation method, b) inference system with sub-clustering method. The black spheres are input variables in the left side and output variables in the right side, and white spheres are the membership functions.

3.4. Accuracy assessment of different model results

The R^2 between the measured and modeled ST using the MLR, ANN, and ANFIS models were 0.58, 0.91 and, 0.95, respectively, indicating the different performances of various models (Figure 8).

The accuracy assessment results showed that the ANFIS model had a better performance than ANN and MLR. This better performance might

be attributed to the simultaneous use of the properties of both the neural network and the Fuzzy inference; thus, ANFIS is able to extract the rules from the observed data. The extracted rules enhance the prediction accuracy. The results revealed that the ANFIS model was able to accurately model ST with the least number of real soil temperature data and inputs for the model in the cold season. The better performance of the ANFIS than the ANN model has been reported by many researchers (Firat and Güngör, 2007; Kurtulus and Razack, 2010).

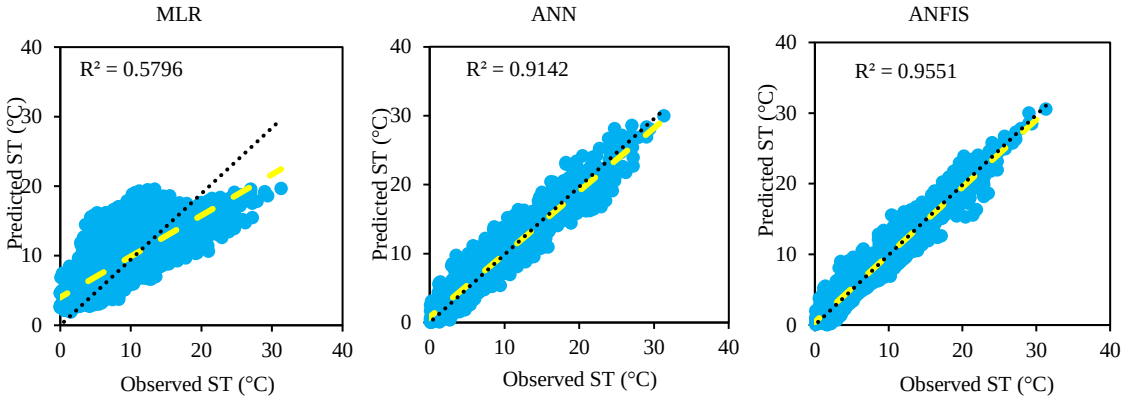

Fig. 8. Comparison of the performance of MLR, ANN, and ANFIS models in ST modeling and comparing with 1:1 line (black dash line)

4. Conclusion

In this study, we developed a model to predict ST using real short time ST data and various predictors such as soil static and dynamic properties. MLR, ANN, and ANFIS models were applied. The results showed that the ANFIS model had a realistic performance in ST modeling using short time data recorded in cold season. We considered the shadow effect on ST for the first time; however, it did not show a significant effect on ST in cold season in the study area. This study showed that the air temperature was the most important environmental parameter with the most significant effect on ST. The ST variation was aligned with AT changes. Temperature fluctuations in the soil surface (5 cm) were more than the subsurface (10 cm). This means that soil depth temperature was less affected by AT than the soil surface temperature. The accuracy of the predictive relationship of ST at 5 cm depth (R^2= 0.96) was more than the 10 cm depth (R^2= 0.92) owing to the faster response of the ST to the AT variations in the surface. By increasing the SM content, a time delay in heat transfer was observed between the soil surface temperature and the air temperature. This is because the most important role of SM is to increase the heat storage capacity of the soil and reduce the intensity of ST fluctuations as it prevents the sudden and sharp changes of temperature in the soil. This role of SM is achieved by increasing the evapotranspiration rate, heat flow in the soil, dissipation of heat down the profile. The results showed that AT, SM, and other soil physical properties could be effective in estimating the ST. The correlation between ST and AT was more significant in the absence of sunlight, which is due to the time delay in heat transfer and temperature fluctuations in the soil. In the present research, there was no significant difference between the sample temperatures in shadow and sun. This is probably attributed to the lower amount of surface incoming solar radiation and the low AT in the winter. Therefore, it is recommended to investigate the difference between the ST in two conditions (shadow and sun) in arid and semi-arid areas in the summer season, where the difference between shadow and sunlight is greater. Such research will also be very useful for understanding the relationship between ST, climate change, and global warming, which has become an increasingly urgent issue over the recent years. It also helps to understand ST behavior and its changes to improve the knowledge on the growth of crops in the soil and other applications. Also, it is recommended that this study be conducted under field conditions for one year, so that the results can be extended to all seasons and natural environments.

References

Abyaneh, H. Z., M. B. Varkeshi, G. Golmohammadi, K. Mohammadi, 2016. Soil temperature estimation using an artificial neural network and co-active neuro-fuzzy inference system in two different climates. Arabian Journal of Geosciences, 9(5); 377.

Al-Kayssi, A., A. Al-Karaghouli, A. Hasson, S. Beker, 1990. Influence of soil moisture content on soil temperature and heat storage under greenhouse conditions. Journal of Agricultural Engineering Research, 45; 241-252.

Alavipanah, S., Q. Weng, M. Gholamnia, R. Khandan, 2017. An analysis of the discrepancies between MODIS and INSAT-3D LSTS in high temperatures. Remote Sensing, 9(4); 347.

Allen, R. G., R. Trezza, M. Tasumi, 2006. Analytical integrated functions for daily solar radiation on slopes. Agricultural and Forest Meteorology, 139 (1-2); 55-73.

Angers, D. A., C. Chenu, 2018. Dynamics of soil aggregation and C sequestration. Soil processes and the carbon cycle, CRC Press: 199-206.

Ay, M., O. Kisi, 2014. Modelling of chemical oxygen demand by using ANNs, ANFIS and k-means clustering techniques. Journal of Hydrology 511: 279-289.

Barman, D., D. K. Kundu, S. Pal, S. Pal, A. K. Chakraborty, A. Jha, S. P. Mazumdar, R. Saha, P. Bhattacharyya, 2017. Soil temperature prediction from air temperature for alluvial soils in lower Indo-Gangetic plain. International agrophysics, 31(1); 9-22.

Beretta, A. N., A. V. Silbermann, L. Paladino, D. Torres, D. Bassahun, R. Musselli, A. García-Lamohte 2014. Soil texture analyses using a hydrometer; modification of the Bouyoucos method. Ciencia e investigación agraria 41(2); 263-271.

Bi, J., M. Zhang, W. Chen, J. Lu, Y. Lai, 2018. A new model to determine the thermal conductivity of fine-grained soils. International Journal of Heat and Mass Transfer, 123; 407-417.

Bilgili, M., 2010. Prediction of soil temperature using regression and artificial neural network models. Meteorology and Atmospheric Physics 110(1-2); 59-70.

Bonakdari, H., H. Moeeni, I. Ebtehaj, M. Zeynoddin, A. Mahoammadian, B. Gharabaghi, 2019. New insights into soil temperature time series modeling; linear or nonlinear? Theoretical and Applied Climatology, 135(3-4); 1157-1177.

Buragohain, M., C. Mahanta, 2008. A novel approach for ANFIS modelling based on full factorial design. Applied soft computing, 8(1); 609-625.

Carman, K., 2008. Prediction of soil compaction under pneumatic tires a using fuzzy logic approach. Journal of Terramechanics, 45(4); 103-108.

Carter, B. J., E. J. Ciolkosz, 1980. Soil Temperature Regimes of the Central Appalachians 1. Soil Science Society of America Journal, 44(5); 1052-1058.

Chatterjee, S., A. S. Hadi 2015. Regression analysis by example, John Wiley and Sons.

Chaudhari, P. R., D. V. Ahire, V. D. Ahire, M. Chkravarty, S. Maity, 2013. Soil bulk density as related to soil texture, organic matter content and available total nutrients of Coimbatore soil. International Journal of Scientific and Research Publications, 3(2); 1-8.

Daddow, R. L., G. Warrington, 1983. Growth-limiting soil bulk densities as influenced by soil texture, Watershed Systems Development Group, USDA Forest Service Fort Collins, CO.

Dai, A., K. E. Trenberth, T. R. Karl, 1999. Effects of clouds, soil moisture, precipitation, and water vapor on diurnal temperature range. Journal of Climate 12(8); 2451-2473.

Davidson, E. A., I. A. Janssens, 2006. Temperature sensitivity of soil carbon decomposition and feedbacks to climate change. Nature, 440(7081); 165.

Delbari, M., S. Sharifazari, E. Mohammadi, 2019. Modeling daily soil temperature over diverse climate conditions in Iran—a comparison of multiple linear regression and support vector regression techniques. Theoretical and Applied Climatology, 135(3-4); 991-1001.

Feng, Y., N. Cui, W. Hao, L. Gao, D. Gong, 2019. Estimation of soil temperature from meteorological data using different machine learning models. Geoderma, 338; 67-77.

Firat, M., M. Gungor, 2009. Generalized regression neural networks and feed forward neural networks for prediction of scour depth around bridge piers. Advances in Engineering Software, 40(8); 731-737.

Firat, M., M. Güngör, 2007. River flow estimation using adaptive neuro fuzzy inference system. Mathematics and Computers in Simulation, 75(3-4); 87-96.

Firozjaei, M. K., M. Kiavarz, O. Nematollahi, M. Karimpour Reihan, S. K. Alavipanah, 2019. An evaluation of energy balance parameters, and the relations between topographical and biophysical characteristics using the mountainous surface energy balance algorithm for land (SEBAL). International Journal of Remote Sensing, 40(13); 5230-5260.

Firozjaei, M. K., O. Nematollahi, N. Mijani, S. N. Shorabeh, H. K. Firozjaei, A. Toomanian, 2019. An integrated GIS-based Ordered Weighted Averaging analysis for solar energy evaluation in Iran; Current conditions and future planning. Renewable Energy, 136; 1130-1146.

Florides, G., S. Kalogirou, 2007. Ground heat exchangers—A review of systems, models and applications. Renewable energy, 32(15); 2461-2478.

Gao, Z., B. Tong, R. Horton, A. Mamtimin, Y. Li, L. Wang, 2017. Determination of desert soil apparent thermal diffusivity using a conduction-convection algorithm. Journal of Geophysical Research; Atmospheres, 122(18); 9569-9578.

Ghuman, B., R. Lal, 1989. Soil temperature effects of biomass burning in windrows after clearing a tropical rainforest. Field Crops Research, 22(1); 1-10.

Hartemink, A.E., J. Bockheim, 2013. Soil genesis and classification. Catena, 104, 251-256.

Hassink, J., A. P. Whitmore, J. Kubát, 1997. Size and density fractionation of soil organic matter and the physical capacity of soils to protect organic matter. European Journal of Agronomy, 7(1-3); 189-199.

Hecht-Nielsen, R., 1992. Theory of the backpropagation neural network. Neural networks for perception, Elsevier; 65-93.

Jackson, M.L., 2005. Soil chemical analysis: Advanced course. UW-Madison Libraries Parallel Press.

Jacovides, C., 1998. Reply to comment on Statistical procedures for the evaluation of evapotranspiration computing models. Agricultural Water Management, 37(1); 95-97.

Kalogirou, S. A., 2013. Solar energy engineering; processes and systems, Academic Press.

Karthika, B., P. C. Deka, 2015. Prediction of air temperature by hybridized model (Wavelet-ANFIS) using wavelet decomposed data. Aquatic Procedia, 4; 1155-1161.

Klute, A., 1986. Methods of soil analysis, part 1 (physical and mineralogical methods), chapter 36, agronomy 9, 901–926. Madison; American Society of Agronomy.

Klute, A., C. Dirksen, 1986. Hydraulic conductivity and diffusivity; Laboratory methods. Methods of soil analysis; part 1—physical and mineralogical methods, 1; 687-734.

Knight, J. H., B. Minasny, A. B. McBratney, T. B. Koen, B. W. Murphy 2018. Soil temperature increase in eastern Australia for the past 50 years. Geoderma, 313; 241-249.

Koçak, K., L. Şaylan, J. Eitzinger 2004. Nonlinear prediction of near-surface temperature via univariate and multivariate time series embedding. Ecological Modelling 173(1); 1-7.

Kome, G.K., Enang, R.K., Tabi, F.O., Yerima, B.P.K, 2019. Influence of Clay Minerals on Some Soil Fertility Attributes: A Review. Open Journal of Soil Science, 9: 155-188.

Kupfersberger, H., G. Rock, J. C. Draxler 2017. Inferring near surface soil temperature time series from different land uses to quantify the variation of heat fluxes into a shallow aquifer in Austria. Journal of hydrology 552; 564-577.

Kurtulus, B., M. Razack 2010. Modeling daily discharge responses of a large karstic aquifer using soft computing methods; artificial neural network and neuro-fuzzy. Journal of Hydrology 381(1-2); 101-111.

Lei, S., J. L. Daniels, Z. Bian, N. Wainaina, 2011. Improved soil temperature modeling. Environmental Earth Sciences, 62(6); 1123-1130.

Li, M., A. C. Lai, 2012. New temperature response functions (G functions) for pile and borehole ground heat exchangers based on composite-medium line-source theory. Energy, 38(1); 255-263.

Liang, L., D. Riveros-Iregui, R. Emanuel, B. McGlynn 2014. A simple framework to estimate distributed soil temperature from discrete air temperature measurements in data-scarce regions. Journal of Geophysical Research; Atmospheres, 119(2); 407-417.

Liao, C.-L., H.-H. Huang, 2012. Study on Shadow Effects of Various Features on Close Range Thermal Images. International Archives of the Photogrammetry, Remote Sensing and Spatial Information Sciences, 39; B5.

Lipiec, J., R. Hatano, 2003. Quantification of compaction effects on soil physical properties and crop growth. Geoderma, 116(1-2); 107-136.

Lu, S., T. Ren, Y. Gong, R. Horton, 2007. An improved model for predicting soil thermal conductivity from water content at room temperature. Soil Science Society of America Journal, 71(1); 8-14.

Luo, D., H. Jin, S. S. Marchenko, V. E. Romanovsky, 2018. Difference between near-surface air, land surface and ground surface temperatures and their influences on the frozen ground on the Qinghai-Tibet Plateau. Geoderma, 312; 74-85.

Maduako, I., Z. Yun, B. Patrick, 2016. Simulation and prediction of land surface temperature (LST) dynamics within Ikom City in Nigeria using artificial neural network (ANN). Journal of Remote Sensing and GIS, 5(1); 1-7.

Mihoub, R., N. Chabour, M. Guermoui, 2016. Modeling soil temperature based on Gaussian process regression in a semi-arid-climate, case study Ghardaia, Algeria. Geomechanics and Geophysics for Geo-Energy and Geo-Resources, 2(4); 397-403.

Mojarrad, F., H. Sadeghi, 2013. Assessing the Relationship between Ground and Soil Temperature at Different Depths; A Case Study of Kermanshah Province.

Moore, L. M., W. K. Lauenroth, D. M. Bell, D. R. Schlaepfer, 2015. Soil water and temperature explain canopy phenology and onset of spring in a semiarid steppe. Great Plains Research, 25(2); 121-138.

Nelson, D., L. E. Sommers, 1982. Total carbon, organic carbon, and organic matter 1. Methods of soil analysis. Part 2. Chemical and microbiological properties, 2; 539-579.

Nelson, R., 1982. Carbonate and gypsum. Methods of soil analysis. Part 2. Chemical and microbiological properties, 181-197.

Onwuka, B., B. Mang, 2018. Effects of soil temperature on some soil properties and plant growth. Adv. Plants Agric. Res, 8; 34-37.

Oyeyemi, K. D., O. Sanuade, M. Oladunjoye, A. Aizebeokhai, A. Olaojo, J. Fatoba, O. Olofinnade, W. A. Ayara, O. Oladapo, 2018. Data on the thermal properties of soil and its moisture content. Data in brief, 17; 900-906.

Ozturk, M., O. Salman, M. Koc 2011. Artificial neural network model for estimating the soil temperature. Canadian journal of soil science 91(4); 551-562.

Park, M., 2018. A Study on Heat-Transfer Characteristics by a Ground-Heating Method. Sustainability, 10(2); 412.

Parsafar, N., S. Marofi, 2011. Estimation of Soil Temperature from Air Temperature Using Regression Models, Artificial Neural Network and Adaptive Neuro-Fuzzy Inference System (Case Study; Kermanshah Region).

Pegalajar, M.C., Sánchez-Marañón, M., Ruíz, L.G.B., Mansilla, L., M. Delgado, 2018. Artificial Neural Networks and Fuzzy Logic for Specifying the Color of an Image Using Munsell Soil-Color Charts. In, International Conference on Information Processing and Management of Uncertainty in Knowledge-Based Systems (pp. 699-709): Springer

Pelletier, C., S. Valero, J. Inglada, N. Champion, G. Dedieu 2016. Assessing the robustness of Random Forests to map land cover with high resolution satellite image time series over large areas. Remote Sensing of Environment, 187; 156-168.

Quattrochi, D. A., J. C. Luvall, 2004. Thermal remote sensing in land surface processing, CRC Press.

Rawls, W., Y. A. Pachepsky, J. Ritchie, T. Sobecki, H. Bloodworth (2003). Effect of soil organic carbon on soil water retention. Geoderma, 116(1-2); 61-76.

Reeves, D., 1997. The role of soil organic matter in maintaining soil quality in continuous cropping systems. Soil and Tillage Research 43(1-2); 131-167.

Ren, X., J. Santamarina, 2018. The hydraulic conductivity of sediments: A pore size perspective. Engineering Geology, 233: 48-54.

Rubio, M., D. Cobos, R. Josa, F. Ferrer, 2009. A new analytical laboratory procedure for determining the thermal properties in porous media, based on the American standard D5334-05. Estudios en la Zona no Saturada del Suelo, 9; 18-20.

Şahin, M., B. Y. Yıldız, O. Şenkal, V. Peştemalcı, 2012. Modelling and remote sensing of land surface temperature in Turkey. Journal of the Indian Society of Remote Sensing, 40(3); 399-409.

Sandholt, I., K. Rasmussen, J. Andersen, 2002. A simple interpretation of the surface temperature/vegetation index space for assessment of surface moisture status. Remote Sensing of environment, 79(2-3); 213-224.

Sanikhani, H., R. C. Deo, Z. M. Yaseen, O. Eray, O. Kisi, 2018. Non-tuned data intelligent model for soil temperature estimation; A new approach. Geoderma, 330; 52-64.

Seber, G. A., A. J. Lee 2012. Linear regression analysis, John Wiley and Sons.

Shaoning, L., J. Wen, Y. Zeng, H. Tian, Z. Su, 2014. An improved two-layer algorithm for estimating effective soil temperature in microwave radiometry using in situ temperature and soil moisture measurements. Remote sensing of environment, 152; 356-363.

Singh, V. K., B. P. Singh, O. Kisi, D. P. Kushwaha, 2018. Spatial and multi-depth temporal soil temperature assessment by assimilating satellite imagery, artificial intelligence and regression based models in arid area. Computers and electronics in agriculture, 150; 205-219.

Stolpe, N., P. Undurraga, 2016. Long term climatic trends in Chile and effects on soil moisture and temperature regimes. Chilean journal of agricultural research, 76; 487-496

Terefe, T., I. Mariscal-Sancho, F. Peregrina, R. Espejo 2008. Influence of heating on various properties of six Mediterranean soils. A laboratory study. Geoderma, 143(3-4); 273-280.

Tsai, C.-c., Z.-s. Chen, C.-t. Duh, F.-w. Horng, 2001. Prediction of soil depth using a soil-landscape regression model; a case study on forest soils in southern Taiwan. PROCEEDINGS-NATIONAL SCIENCE COUNCIL REPUBLIC OF CHINA PART B LIFE SCIENCES, 25(1); 34-39.

Walia, N., H. Singh, A. Sharma, 2015. ANFIS; Adaptive neuro-fuzzy inference system-a survey. International Journal of Computer Applications, 123(13).

Wang, B., T. Zha, X. Jia, B. Wu, Y. Zhang, S. Qin, 2014. Soil moisture modifies the response of soil respiration to temperature in a desert shrub ecosystem. Biogeosciences, 11(2); 259-268.

Wang, X., C.H. Benson, 2018. Constant-head constant-volume hydraulic conductivity testing of porous materials. Geoenvironmental Engineering; 69-81.

Weng, Q., M. K. Firozjaei, M. Kiavarz, S. K. Alavipanah, S. Hamzeh, 2019. Normalizing land surface temperature for environmental parameters in mountainous and urban areas of a cold semi-arid climate. Science of The Total Environment, 650; 515-529.

Weng, Q., M. K. Firozjaei, A. Sedighi, M. Kiavarz, S. K. Alavipanah, 2019. Statistical analysis of surface urban heat island intensity variations; A case study of Babol city, Iran. GIScience and Remote Sensing 56(4); 576-604.

Yener, D., O. Ozgener, L. Ozgener, 2017. Prediction of soil temperatures for shallow geothermal applications in Turkey. Renewable and Sustainable Energy Reviews, 70; 71-77.

Zhang, D., Z.-L. Li, R. Tang, B.-H. Tang, H. Wu, J. Lu, K. Shao, 2015. Validation of a practical normalized soil moisture model with in situ measurements in humid and semi-arid regions. International Journal of Remote Sensing, 36(19-20); 5015-5030.